EFFECT OF THE SIZE OF MULTI-LAYER SPACER CONFIGURATION ON MEMBRANE PERFORMANCE: A CFD STUDY

LINA NABILAH BINTI LUQMAN LOKE

BACHELOR OF CHEMICAL ENGINEERING

UNIVERSITI MALAYSIA PAHANG

DECLARATION OF THESIS AND COPY RIGHT

Author's Full Name : <u>LINA NABILAH BINTI LUQMAN LOKE</u>

Date of Birth : <u>6/5/1995</u>

Title : <u>EFFECTOF THE OF SIZE OF MULTILAYER</u>

<u>SPACER CONFIGURATION ON MEMBRANE</u>

<u>PERFORMANCE : A CFD STUDY</u>

Academic Session : <u>16/17</u>

I declared that this thesis is classified as:

☐ **CONFIDENTIAL** (Contains confidential information under the Official Secret Act 1972) *

☐ **RESTRICTED** (Contains restriction information as specified by the organization where research was done) *

■ **OPEN ACCESS** I agree that my thesis to be published as online open access (Full text)

I acknowledge that University Malaysia Pahang reserve the right as follows:

1. The Thesis is the Property of University Malaysia Pahang.

2. The Library of University Malaysia Pahang has right to make copies for the purpose of research only.

3. The Library has the right to make copies of the thesis for academic exchange.

Certified By:

_____   _____
(Student's Signature)   (Supervisor's Signature)

<u>LINA NABILAH LUQMAN</u>   <u>Dr. LIANG YONG YOEW</u>
950506-10-5598   Name of Supervisor
Date: 20/06/2017   Date:20/06/2017

NOTES : *If the thesis is CONFIDENTIAL or RESTRICTICTED, please attach with the letter from the organization with period and reasons for confidentiality or restriction

SUPERVISOR'S DECLARATION

We hereby declare that we have checked this thesis and in our opinion, this thesis is adequate in terms of scope and quality for the award of the degree of Bachelor of Chemical Engineering.

Signature   :
Name of main supervisor : Dr. LIANG YONG YOEW
Position   : LECTURER CHEMICAL ENGINEERING
Date   : 20 JUNE 2017

STUDENT'S DECLARATION

I hereby declare that the work in this thesis is my own except for quotations and summaries which have been duly acknowledged. The thesis has not been accepted for any degree and is not concurrently submitted for award of other degree

Signature   :
Name   : LINA NABILAH BINTI LUQMAN LOKE
ID Number   : KE 14046
Date   : 20 JUNE 2017

Dedicated to my family, friends and lecturers.

ACKNOWLEDGEMENT

ABSTRACT

The spiral wound membrane (SWM) module are the membrane technology for water treatment and the Reverse Osmosis (RO) membrane process is currently leading method and implemented through SWM. SWM module formed by two neighbouring membrane sheets separated by a thin net-type spacer where the separation take place. It come in multiple configurations with different spacer geometry, membrane types and size. Moreover, concentration polarization is strongly affect the performances of separation process. Spacer will reduce the extent of concentration polarization because of the enhanced wall shear thus increase the flux of the membrane. Besides, fouling also result of the concentration polarization. Fouling will increase as the concentration polarization increase then result in loss of permeate flux. Therefore, the objective of this study is to investigate the effect of the size of multilayer spacer configuration on permeate flux and concentration polarization. In the investigation, we want to reduce the concentration polarization by using difference geometry multilayer spacer configuration. Besides, ANSYS Fluent v16.2 is used to develop the 3D multilayer spacer, CFD modelling and flow of simulation.

ABSTRAK

Modul lingkaran membran adalah teknologi membran terkini untuk rawatan air dan proses osmosis berbalik adalah kaedah utama dan dilaksanakan melalui modul lingkaran membran. Modul lingkaran membran dibentuk oleh dua lembaran membran bersebelahan yang dipisahkan oleh peruang lapisan nipis dimana proses pemisahan berlaku. Ia boleh datang dalam pelbagai konfigurasi dengan geometri peruang lapisan yang berbeza, jenis membran dan saiz. Selain itu, kepekatan polarisasi amat berkait dengan prestasi proses pemisahan. Penapis akan mengurangkan tahap kepekatan polarisasi kerana dinding ricih dipertingkatkan sekali gus meningkatkan fluks membran. Selain itu, kekotoran terkumpul juga menyebabkan kepekatan polarisasi bertambah. Kekotoran terkumpul akan meningkat kerana peningkatan kepekatan polarisasi, kemudian menyebabkan kehilangan fluks. Oleh itu, objektif kajian ini adalah untuk mengkaji kesan pada peresapan fluks dan polarisasi yand disebabkan oleh saiz perubahan saiz spacer berkonfigurasi tiga lapisan. Dalam kajian ini, kita mahu mengurangkan kepekatan polarisasi dengan menggunakan konfigurasi geometri peruang lapisan yang berbeza . Selain itu, Ansys v16.2 Fluent digunakan untuk menghasilkan peruang tiga lapisan dalam 3 dimensi, model CFD dan aliran simulasi.

LIST OF ABBREVIATIONS AND SYMBOLS

SWM	Spiral Wound Membrane
RO	Reverse Osmosis
CFD	Computational Fluid Dynamic
GCI	Grid Independence Index
Re	Reynold number
R	refinement ratio
e	relative error
N_{fine}	number of fine grids
N_{coarse}	number of course grids
(η)	dimensional number
ρ	density
v	velocity
d	diameter
μ	viscosity
ht	height of top layer spacer
hm	height of middle layer spacer
hb	height of bottom layer spacer
df	Spacer diameter
$h$ch	Height of geometry
lm	Length of 1 subunit spacer

CHAPTER 1

INTRODUCTION

Reverse osmosis (RO) is one of the separation process and currently implemented through spiral wound membrane (SWM). Spacer reduce the extent of concentration polarization because of the enhanced wall shear rates (Hassan, Al-Sofi et al. 1998). Since SWM can easily be created in different configurations, different size and angle of spacer are used to compare the membrane performance (Koutsou and Karabelas 2015). Besides, multilayer spacer configuration also will five different effect towards the membrane performances. Thus, the objective of this research is to investigate the effect of the size of multilayer spacer on membrane performance. The scope of this research included to performed mesh independence study to ensure the amount of the error associated with the grid is less than 10%.

Concentration polarization has long been identified as a major problem that deteriorates the performance of RO systems (Schwinge, Wiley et al. 2002). Concentration polarization are strongly affect the performances of separation process. However, this phenomenon is still not well understood especially in practical Spiral Wound Module (SWM), where spacer is an essential part to form the feed channel (Lopes, Chavez et al. 2012). The purpose of this study was to study concentration polarization in spacer filled RO system and to quantify the impact of feed spacer on concentration polarization and membrane performance. There are a numerous study of CFD modelling on membrane spacer geometry performance, but there are still no research on effect when there are a variation in the multilayer spacer geometry. Then those option was the focus in this research.

To run the simulation, there are five step need to be done. First, develop the geometry in their own variation of spacer size for all cases by using Ansys Workbeach v16.2. In this research we do have five cases of different spacer size to be compared. The geometry are

developed in 3D modelled and stick in same angle between spacer which is 45°. Naming each part of the geometry and add inflation before mesh it. Check the verification and validation of the mesh model by calculate the grid independence index (GCI). The GCI must below 10%. Then set up the boundary through CFX pre. After set up boundary condition, the simulation can start to run. The result is concentration polarization, pressure drop, shear wall, flux and velocity profile.

1.1   Background of the study

The spiral wound membrane (SWM) module are the membrane technology for water treatment. The Reverse Osmosis (RO) membrane process is currently leading method and implemented through SWM (Koutsou and Karabelas 2015). Because of its construction, it can easily be created in different configurations, with various length, diameter and membrane material (Hassan, Al-Sofi et al. 1998). The most important flow in the SWM module is that formed by two neighbouring membrane sheets separated by a thin net-type spacer (Bowen and Mukhtar 1996). This is where the separation take place.

Separation process are related to the concentration polarization. In membrane process accumulation of rejected species near the feed side of the membrane which is concentration polarization causes reduction of permeate flux (Li, Meindersma et al. 2002). To have better flux, concentration polarization need to be reduce. Besides, fouling also result of the concentration polarization. Fouling will increase as the concentration polarization increase then result in loss of permeate flux (Ochando-Pulido, Verardo et al. 2015). As a short term effect, fouling leads to an increase in the energy cost to maintain the target of the permeate production.

the feed channel spacer to provide turbulent and create space between membrane sheets (Schwinge, Wiley et al. 2002). It form uniform flow of water to the membrane surface. Then, the sheet combined with permeate channel spacer and provide open flow channel to the permeate spacer at high pressure. Furthermore, during high pressure RO desalination, additional normal stresses are experienced by the permeate spacer due to high pressure prevailing at the retentate side.
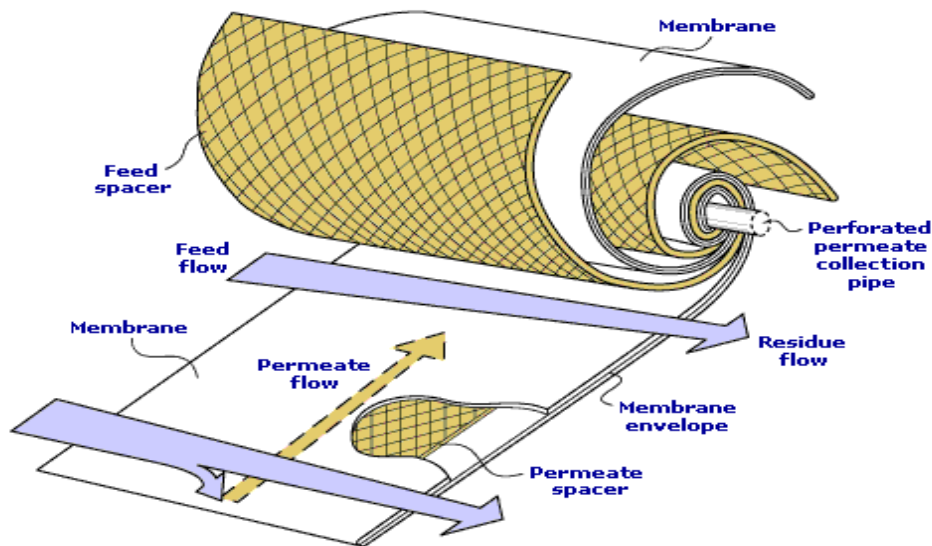
Fig 1.1: A view of Spiral Wound Membrane (SWM) module (Schwinge, Wiley et al. 2002).

1.2   Motivation

On average, spacer reduced the extent of concentration polarization because of the enhanced wall shear rates (Subramani, Kim et al. 2006) thus increase the flux of the membrane. In most studies, spacer geometry characteristics are conventional spacer which are zigzag, cavity and submerged geometry. SWM elements come in multiple configurations with different spacer geometry, membrane types and size. This elements allow it to fit a multiple applications.

Traditionally, SWM are equipment for mesh or conventional type spacer (Schwinge, Wiley et al. 2000),(Fimbres-Weihs and Wiley 2010). There are different in flow of water through the membrane when the spacer geometry are change (Ranade and Kumar 2006). In addition, recent studies suggest that certain flow characteristic lead to increase in mass transfer (Fimbres-Weihs and Wiley 2010). For example, flow towards the membrane wall and the wall shear perpendicular to the bulk flow direction. Thus, multilayer spacer need to be compared with single layer spacer whether multilayer gives better effect towards the flow of water.

1.3   Problem Statement

As a phenomenon inherently associated with membrane separations, concentration polarization has long been identified as a major problem that deteriorates the performance of RO systems (Schwinge, Wiley et al. 2002). Concentration polarization are strongly affect the performances of separation process. However, this phenomenon is still not well understood especially in practical Spiral Wound Module (SWM), where spacer is an essential part to form the feed channel (Lopes, Chavez et al. 2012). The purpose of this study was to study concentration polarization in spacer filled RO system and to quantify the impact of feed spacer on concentration polarization and membrane performance.

1.4   Objectives

The objective of this study is to investigate the effect of the size of middle spacer of multilayer spacer configuration on permeate flux and concentration polarization.

1.5   Scopes of Study

The following are the scopes of this research:

1) To perform a mesh impendence study to ensure the amount of error associated with the grid within an acceptable error (5-10%).
2) To use CFD to investigate the effect of the size of the multilayer spacer configuration on concentration polarization and permeate flux.

CHAPTER 2

LITERATURE REVIEW

2.1   Membrane Process

Membrane separation process were very important to the separation industry. Membrane separation often performs at greatest efficiency when the feed in pressurised (Karode and Anderson 2004). Some of the membrane separation process are ultrafiltration, nanofiltration, and reverse osmosis (RO). These three process are different in their pore size, pressure and the separation mechanism.

Ultrafiltration was lead to a separation through semipermeable membrane. These membrane have a pore size of around 0.01 microns. It would remove larger particle and some viruses. Ultrafiltration are typically used to separate protein from buffer component for buffer exchange, desalting or concentration (Kimura 1991). Another membrane process is nanofiltration. Nanofiltration has a pore size of 0.001 microns. The pore dimensions are controlled by pH and temperature. This filter removes nearly all viruses, a range of salt and most of the organic molecules (Kowalska 2014).

Next process that we are focusing is reverse osmosis (RO) which has pore filter size around 0.0001 microns. The largest and most important application of RO is the separation of pure water from sea water and brackish water (Greenlee, Lawler et al. 2009). Brackish water may result from mixing of sea water and fresh water. Seawater or brackish water is pressurized against one surface of the membrane. It cause the transport of salt water across the membrane and emergence of potable drinking water from low pressure side (Pasternak 1992). This process is currently the undisputed leading method for water treatment.

Although current material and chemical engineering technology has made it possible to manufacture membranes with excellent performances, example, high permeability, low fouling potential and high rejection for pressure driven membrane system there are still some unsolved practical problems that retard the process of popularization. Concentration polarization and membrane fouling are the most important twin problem in most practical RO membrane system (Tang, She et al. 2010).

The Spiral Wound Membrane (SWM) module is the basic module for desalination and water treatment technology. RO is a process of forcing a solvent from higher solute concentration region to lower solute concentration region (Lee, Arnot et al. 2011). Pressure is applied to overcome the osmotic pressure.
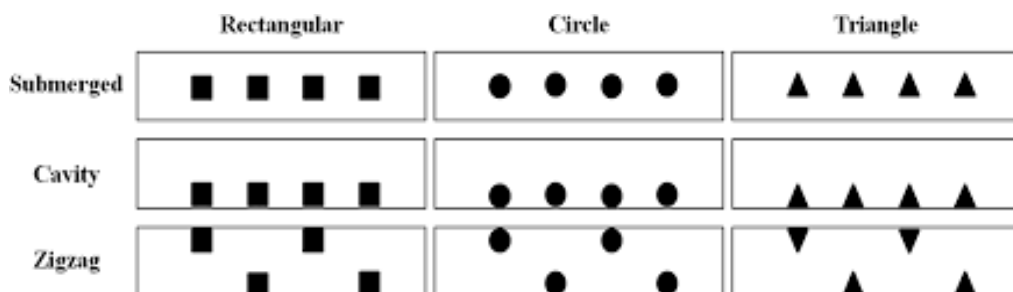
2.2   Spacer Configuration

In most RO modules, feed spacer is an essential part to keep membranes apart from the feed channel. Although the effect of spacer filaments on hydrodynamics parameters such as velocity, wall stress and pressure drop have been studies and reported (Saeed, Vuthaluru et al.). A quantitative link between the spacers and concentration polarization is still unavailable. This makes it extremely difficult to optimize the spacer for a better system performance.

Spacer attached to a membrane can effect concentration boundary layer in a membrane channel in two ways. For the membrane attached to the transverse spacer which are zigzag and cavity configuration, concentration boundary layer is disrupted periodically by the spacer and induced recirculation (Koutsou, Yiantsios et al. 2007). In an interval between two neighbouring spacer, the concentration boundary layer grows in two opposite direction. One approaching the upstream spacers due to reversed flow and the other approaching the downstream spacers. For membrane region opposite to the transverse spacers, concentration boundary layer is periodically compressed by the constricted passage between transverse spacers and the opposite membrane. For submerged configuration spacer, there are no concentration boundary layer disruption because the transverse spacer are not attached to the membrane. The recirculation flow

formed in the downstream of ach filament is only restricted in the central part of the channel and no reversed flow is developed near the membrane surfaces.

Spacer geometry was found to have significant impact on concentration polarization. Membrane performance also affected by spacer configuration and mesh length. The combination of concentration boundary layer can result in the greatest concentration polarization, as in this case is zigzag configuration (Schwinge, Wiley et al. 2004). Usually, zigzag configuration provided the best permeate flux enhancement to improving the performance of the RO process (Amokrane, Sadaoui et al. 2016). For submerged configuration, concentration polarization and permeate flux enhancement are mainly achieved by concentration boundary layer compression (Amokrane, Sadaoui et al. 2016),(Schwinge, Wiley et al. 2000). This also applies to the membrane opposite to the transverse spacer in cavity configuration. For cavity configuration, if the membrane is attached to the transverse spacer, concentration polarization and permeate flux would be mainly affected by concentration boundary layer disruption. For zigzag configuration, these two mechanism are combined.

There was an optimum mesh length with cavity and submerged configuration for maximizing permeate flux enhancement. Decreasing mesh length may lead to increase in pressure loss especially for zigzag configuration, and may lead to permeate flux decline. The arrangement of zigzag spacer was under alternate, while for cavity spacer was parallel at the bottom and parallel at the middle for the submerged spacer. Figure 2.2 shows the configuration for zigzag, cavity and submerged spacer.

Fig 2.2: Configuration of the different spacer membrane geometry (Schwinge, Wiley et al. 2004).
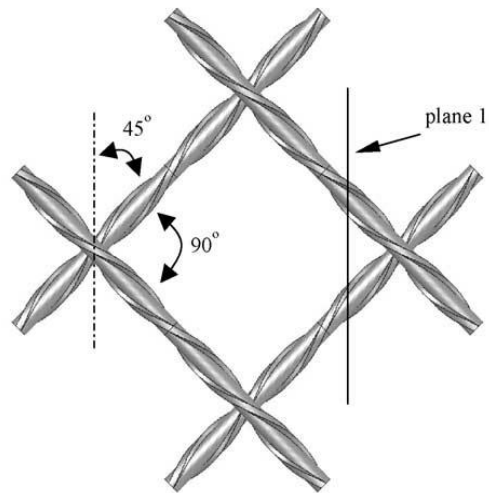
2.2.1   Two layer spacer

Based on (Fimbres-Weihs and Wiley 2008), the geometries analysed are the variations of the 2D zigzag spacer arrangement. A basic zigzag geometry was chosen because it presents the most similarities to spacers used in real membrane modules. The df/$h$ch ratio was varied from 0.6 down to 0.3, while keeping the ratio of lm/df at a constant value of 6.667. As the filament diameter is decreased, the cross-section of the channel that is obstructed is also decreased. It is therefore expected that for lower filament diameter to channel height ratios the friction factor will be lower, approaching the value for an empty channel.

The effect of filament diameter on Sherwood number is more complex than its effect on the friction factor. For empty channels, the Sherwood number for flow with a fully developed concentration profile does not depend on the Reynolds number. However, for spacer-filled channels the Sherwood number increases as the Reynolds and Power numbers are increased, as a consequence of increased boundary layer destabilization at higher Reynolds numbers. At low Reynolds numbers, where no boundary layer separation occurs and creeping flow conditions are prevalent, the Sherwood number will be lower for the spacer-filled channels than for the empty channel as a result of the spacer filaments covering the membrane surface and reducing the available mass transfer.

For empty channels, entrance region effects caused by the developing boundary layer result in a higher Sherwood number near the channel inlet (Balster, Pünt et al. 2006). As the distance from the channel inlet is increased, the Sherwood number eventually reaches asymptotic value. Since further increases in channel length do not affect the Sherwood number, the concentration profile is considered to be "fully developed".

For a given energy loss, the Sherwood number is always higher for spacer filled channels than for an empty channel. In addition the empty channel requires less energy to attain a fully developed concentration profile than the spacer-filled geometries tested. This is to be expected given that pressure drop for the empty channel is significantly lower than for the spacer-filled cases. The geometries with a higher

Sherwood number under fully developed concentration profile conditions will usually have a higher Sherwood number at any given value for the energy loss throughout the entire length of the channel.

Fig 2.2.1: An illustration of two layer spacer (Fimbres-Weihs and Wiley 2008)
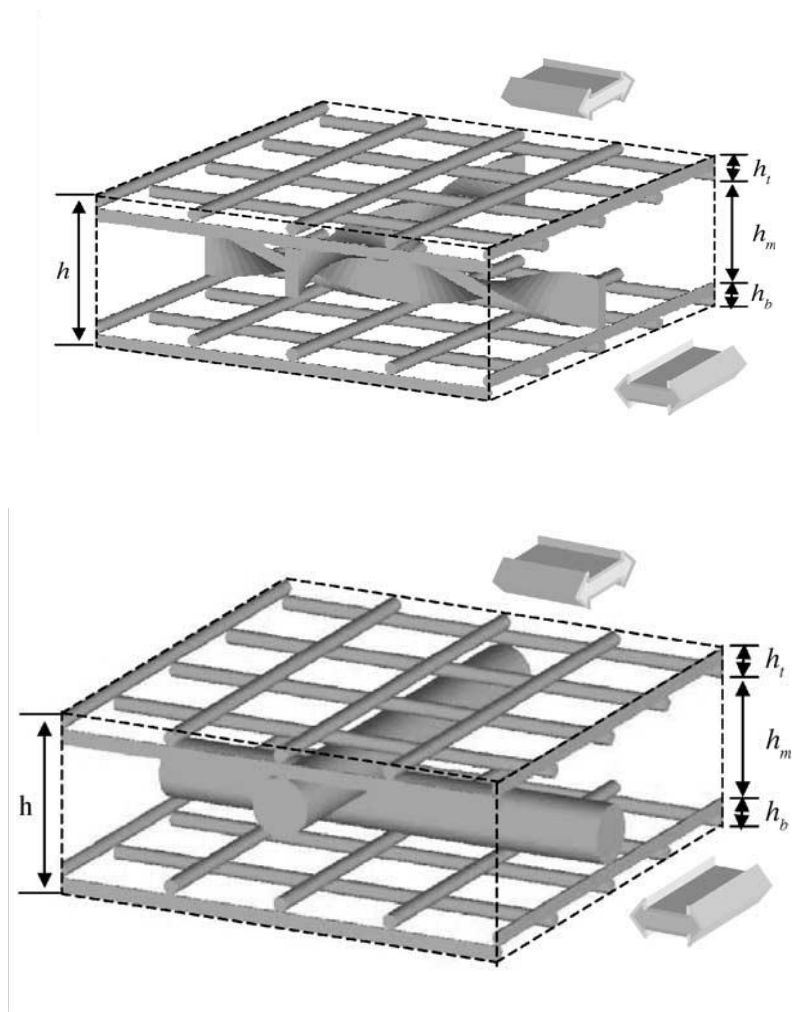
2.2.2   Multilayer spacer

Based on (Balster, Pünt et al. 2006), multilayer spacers have three distinct layer. The multilayer spacer created by the combination of the middle spacer with round filaments and a flow attack angle of 45◦ with two thin net spacers on the outside showed the best performance. In the case of a multi-layer spacer, the middle spacer diverts the flow from the bulk to the channel walls, where the thin net spacers create of a mix of longitudinal and transversal vortices close to the membrane, decreasing the boundary layer thickness. The creation of swirling flows by the middle spacer seems to reduce the effect of the outside net spacers. Therefore, no modified filament structures are needed for the middle spacer.
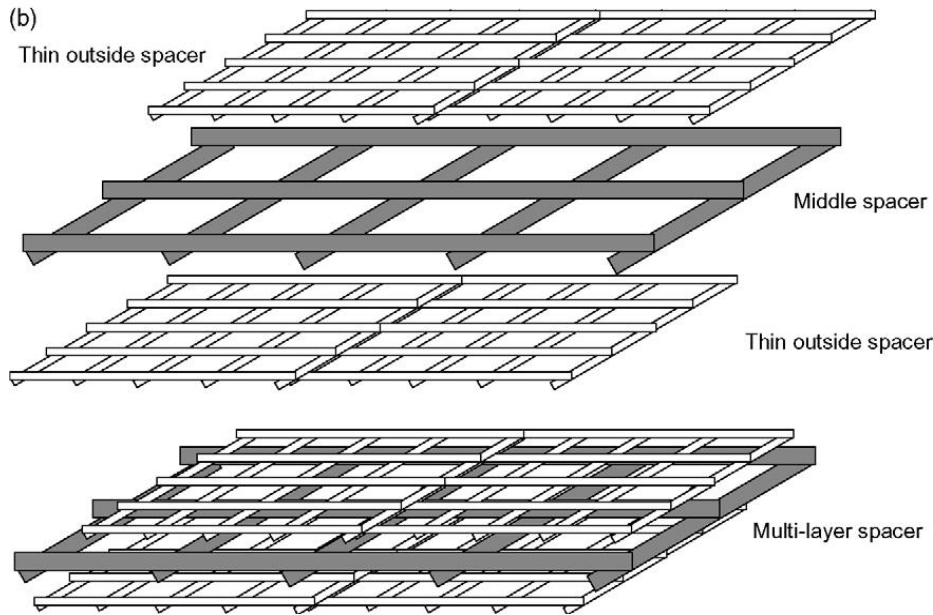
Fig 2.2.2a: An illustration of multilayer spacer (Balster, Pünt et al. 2006).

Based on (Li, Meindersma et al. 2005), The layers close to the channel walls generate swirling flows, and the middle layer diverts the flow from bulk to the channel walls. The geometric parameters needed for characterization of multi-layer structures are the height of each layer (ht for the top layer, hm for the middle layer, and hb for the bottom layer). The comparison based on performance of this spacer with the optimal non-woven spacer indicates that the performance of multi-layer spacer is very promising. Its average Sherwood number is about 30% higher than that of the optimal non-woven spacer at the same cross-flow power consumption whereas the cross-flow power consumption is only about 40% of the optimal at the same average of Sherwood number. Therefore, multilayer spacer is more effective.

In order to reduce the energy consumption, thinner middle spacers were also studied. The best multi-layer, resulted in the same mass transfer enhancement as the multi-layer at 30 times lower cross-flow power consumption. This novel multi-layer spacer showed a 20% higher mass transfer compared to a standard non-woven optimum net spacer at the same cross-flow power consumption. For an industrial application of this multi-layer spacer, a further reduction of the spacer thickness below 2mm would be necessary.

Fig 2.2.2b: A view of multilayer spacer (Li, Meindersma et al. 2005)

2.3 Computational Fluid Dynamic (CFD) in membrane system

Steady state modelling of CFD was the early efforts to model the flow field through membrane sheet. Before proceeding further, a brief overview will be made of simulation approaches not based on the foregoing scale separation (Fletcher and Wiley 2004). Dynamic model development is a discussion refers to the absence of any type of material accumulation in the membrane elements.

It provides a qualitative prediction of fluid flows by means of mathematical modelling, numerical methods and software tools. Numerical simulation in fluid flows enable architects to design comfortable and safe living environments, chemical engineer to maximize the yield from their equipment, petroleum engineer to devise optimal oil recovery strategies and etc (Ndinisa, Wiley et al.). Besides, CFD is used to solve and analyse the problem that involve fluid flows and shear stressed (Williams, Saini et al. 2002). The many reason CFD consulting is being widely used today such as great reduction in time and cost in new design, gives reliable result, provide exact and details information and easily explore and compared design alternatives.

2D studies have provided valuable insights into the interactions between the flow and mass transfer, SWM modules for real world applications are 3D by nature (Katsoufidou, Yiantsios et al. 2007). However, obtaining 3D numerical solutions for flow problems using CFD requires many more computations than those required for 2D flows. 2D simulations require a number of mesh elements of the order of tens to thousands, 3D simulations have been reported to require millions to tens of millions of mesh elements when incorporating mass transfer (Katsoufidou, Yiantsios et al. 2007).

2.4 Mesh Independent Study

The accuracy of CFD simulations result is depends on the mesh quality. Mesh independence study is the verification and validation of the mesh model. The purpose of mesh independence study is to ensure the computational code is accurately solving the system of partial differential equations that the transported equations defined. Grid independence index (GCI) is use to estimate the error associated with the grid. GCI for fine and course can be calculated by:

$$CGI_{fine} = \frac{3|e|}{R^{\eta} - 1} \qquad (2.4.1)$$

$$CGI_{coarse} = \frac{3|e|R^{\eta}}{R^{\eta} - 1} \qquad (2.4.2)$$

Refinement ratio ($R = N_{fine} / N_{coarse}$) is the ratio of mesh elements between the fine and coarse grids, $e = (F_{coarse} - N_{fine} / N_{fine})$ is the relative error for the calculation of the integral function, and the dimensional number (η) is equal to the number of dimensions modelled (2 for 2D and 3 for 3D). Verification can thus be carried out by successively increasing spatial and/or temporal resolution until the GCI for the fine mesh falls below an acceptable error level (less than 10%).

2.5 Gap Analysis

Although there are numerous study of CFD modelling of membrane spacer geometry on performance (Peng, Lee et al. 2015), the study into the multilayer spacer configuration is scarce (Akhilesh, Srijani et al. 2013). No study has been done to investigate the effect of size of middle layer spacer of multi-layer spacer configuration on concentration polarisation and shear stress. Those options are the focus of this thesis.

CHAPTER 3

MATERIALS AND METHODS
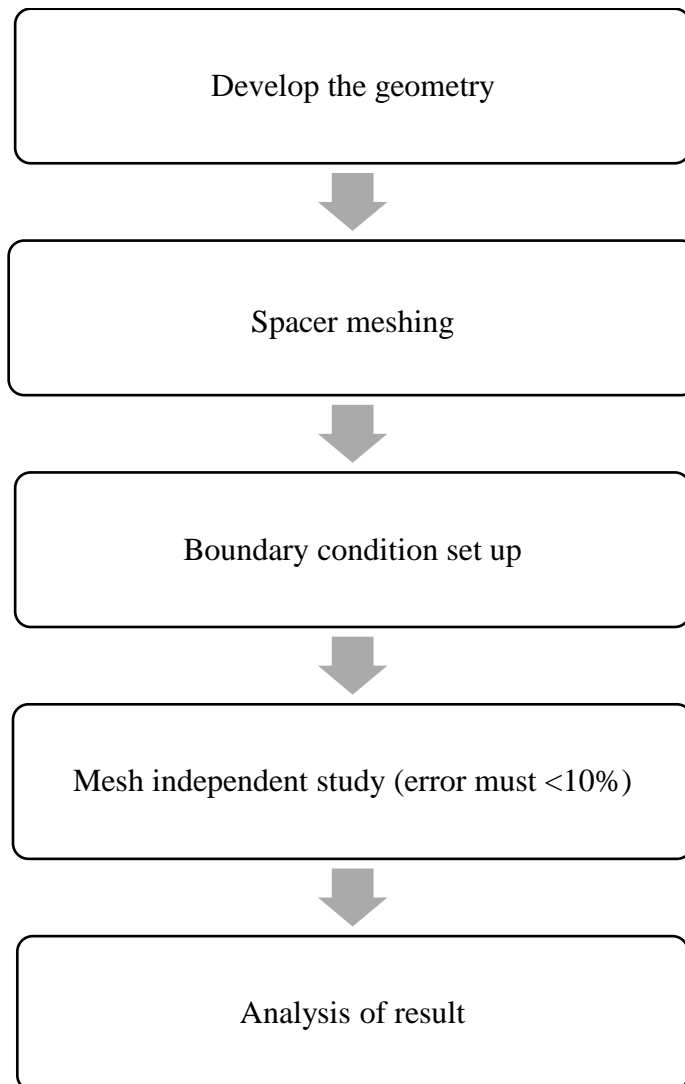
Figure 3.0: A flowchart of simulation.

3.1 Develop the Geometry

In this research 3D geometries was developed because greater mass transfer enhancement was found for 3D geometries modeled (Fimbres-Weihs and Wiley 2007), (Fimbres-Weihs and Wiley 2010). There are four case of geometry to be compared. The three case are geometry with same df/hch of top and bottom spacer which is 0.4 while the df/hch of middle spacer are 0.3, 0.4 and 0.5. One more case are 0.5 df/hch for top and bottom spacer while 0.4 df/hch for middle spacer. We stick the orientation are at 45° orientation for all cases. The example characteristic of the meshing is narrow zigzag spacer-filled channel with the increasing of the height/depth ratio in filled the entire channel height(Fimbres-Weihs and Wiley 2007). Arrangement type of zigzag are used in this study for all cases.

Lm middle spacer = 9.12mm
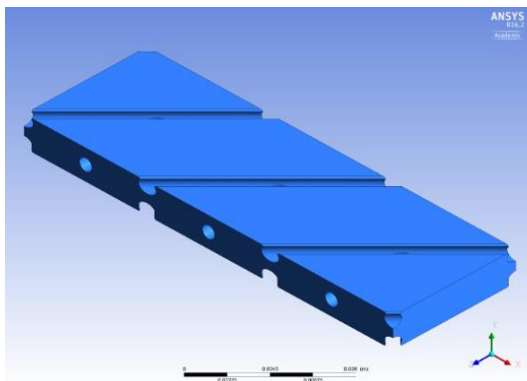
Lm top and bottom spacer = 6.45mm
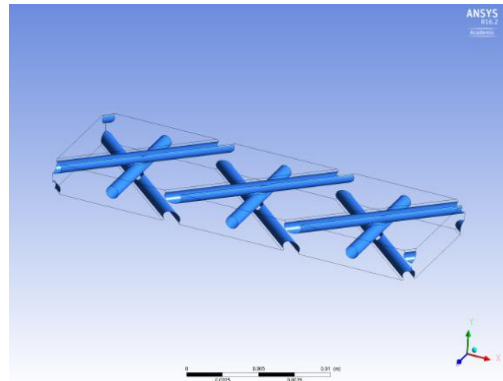
Depth = 9.12 mm

Angle = 45°

hch = 2.28mm

$$\frac{dh}{hch} = 4$$

$$\frac{df}{hch} \ (4 \ cases) = middle \ spacer \ (0.3, 0.4, 0.5) \ and \ top \ and \ bottom \ spacer \ (0.5)$$

Besides, the overlapping between top and bottom spacer with middle spacer is calculated by 0.4df, that value are distance between centre of top and bottom spacer to the membrane.

Fig 3.1(a) Ilustration of 3D geometry   **Fig 3.1(b)** Ilustration of multilayer spacer

3.2 Spacer Meshing

The spacer meshing is the distance between the filament cross section. The spacer meshing was set up and generated through ANSYS Workbench 16.2. The physics preference is set for CFD as the fluid flow through the geometry will be analysed using fluent, under the mesh setting. To account the geometry spacer filaments, the advance minimum size, maximum size face and maximum size function are being used to curvature. The relevance centre was set to fine high smoothing, fine angle centre and slow transition. The number of element of mesh used in this research was around 14 million for all cases. Besides, the mesh was generated in y-direction (Fimbres-Weihs and Wiley 2007).

3.3 Boundary Condition Setup

ANSYS Fluent v16.2 was used to simulate a flow through the spacer filled channel geometry and CFX solver is used to analyze the steady state condition of the fluid flow. The effects of gravity were ignored and velocity formulation was set to relative. The viscous laminar model was used to simulate the flow as the fluid Reynolds number tested is relatively low. For the geometry's boundary conditions, the channel inlet of the geometry was defined as a velocity inlet. Here, the velocity of the flow was varied by manipulating the flows Reynolds number, Re**.** Density of water is 998.2 kg/m and the viscosity is 0.001003 kg/(m.s).

3.4   Mesh Independence Study

Mesh independence study is the verification and validation of the mesh model. The accuracy of CFD simulations result is depends on the mesh quality. The purpose of mesh independence study is to ensure the computational code is accurately solving the system of partial differential equations that the transported equations defined. This part is the most important part of the research. Grid independence index (GCI) is use to estimate the error associated with the grid. How to calculate the GCI error has been stated before in subtopic 2.4.

3.5 Analysis of Result

Data were obtained from a sampling line positioned at the centre of the main spacer filled channel in CFD-Post. The analysis consists of the concentration polarization, velocity profile, pressure drop and flux. In the discussion, we have compared the average of x vorticity to z vorticity, shear wall stress ratio of z to x direction, fanning fraction and the area average fluid velocity.   Since we have four cases of different size of spacer. So we compared membrane performance between different middle size spacer and then between different top and bottom size of spacer.

CHAPTER 4

RESULTS AND DISCUSSION

4.1   Feed Spacer Geometry

In this research, there are four cases of different spacer size geometry to be compared. All cases are created in partially woven. For each elemental unit, the flow is assumed to be laminar with Reynold Number, N_{re}=200 and steady state. Elemental unit consists of five type of boundary which are inlet, outlet, side wall, spacer and membrane wall. The elemental unit that we develop with different configuration of size of middle, top and bottom spacer. Each geometry has same ratio of height and different ratio of spacer diameter:

$$hch = 2.28mm, \quad \frac{dh}{hch} = 4$$

	(a)	(b)	(c)	(d)
$\frac{df}{hch}$ middle spacer	0.4	0.3	0.5	0.4
$\frac{df}{hch}$ top and bottom spacer	0.4	0.4	0.4	0.5

Table 4.1: Size of the spacer

(a)   (b)

(c)   (d)
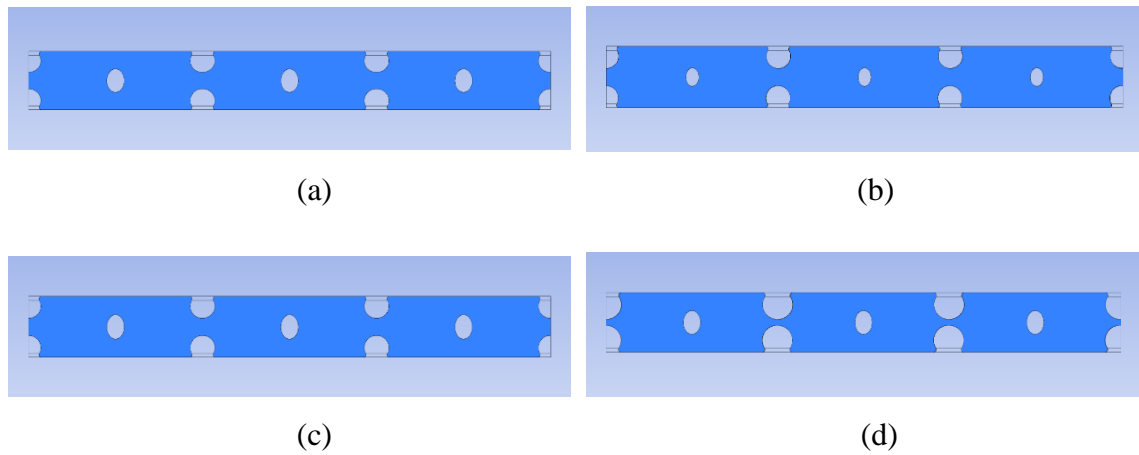
Figure 4.1: Different multilayer spacer size

The spacer are arranged in a zigzag arrangement since this configuration was an optimum mesh length with cavity and submerged configuration for maximizing permeate flux enhancement (Amokrane, Sadaoui et al. 2016),(Schwinge, Wiley et al. 2000).. Decreasing mesh length may lead to increase in pressure loss especially for zigzag configuration, and may lead to permeate flux decline. Thus, better membrane performance will be achieve. So now, we only need to study which size of spacer will provide greater mass transfer enhancement.

4.2   Mesh Independence Analysis

Mesh independence analysis is the most important part. This part is to check the validation of the meshing. To have a reliable result, we need to ensure that the error within the grid must below 10%. There are two type of meshing which are fine and course. Since we have four cases of different size of spacer to being compared that consists of df/hch of middle spacer of 0.3, 0.4 and 0.5 with a same size of top and bottom spacer, and df/hch of top and bottom spacer of 0.5 with middle size of 0.4. The mesh independence test was performed for each of the geometry to calculate Grid Convergence Index (GCI) percentage. The mesh quality was refined by increasing the number of elements of each geometry and GCI percentage of fanning friction and average velocity across the filament channel were compared between finer and coarser mesh.

Based on the GCI percentage for average velocity across the filament and the fanning friction, it can be observed that increase the number of element from courser mesh to finer mesh for all configuration spacer will reduce the GCI value for both average velocity and fanning friction. It means that the error decrease when number of element is increase. Before we run mass transfer, we need to minimize the error because it occurs very sensitive separation process. Therefore, the result produced by the meshes with large number of element and lower GCI values were assumed to be mesh independence.

The value of average velocity across the filament and the average fanning friction decrease when the number of element increase. But the value will constant at one value even though we increase the number of elements. This is because the number has achieved saturated number of mesh. Courser meshing A coarse mesh will require less computational resources to solve and, while it may give a very inaccurate solution. That why we need the fine meshing to reduce the error during mass transfer.

| Geometry	Number of element	GCI Fanning Friction (%)	GCI average Velocity (%)
	10261732	-	-
	14262954	13.664	29.845
45° Spacer Filament	20789640	4.412	9.637
	29377890	2.983	4.310
	40000000		

Table 4.2: Grid Convergence Index with different number of element.

## 4.3 Effect of Different Size of Spacer on Fluid Velocity Across the Domain Filaments

Fluid velocity was analysed with the same Reynold number which is 200. The Velocity profile was compared by four different size of middle, top and bottom spacer. By using the course mesh, the simulation is run using CFX to monitor the velocity profile across the filament channel. The results were analyzed by comparing the velocity profile across the filament channel showed in figure 5, 6, 7 and 8.
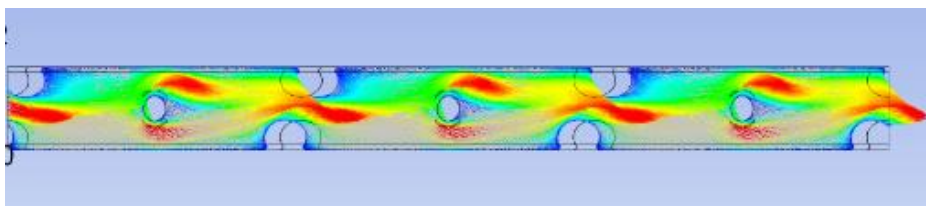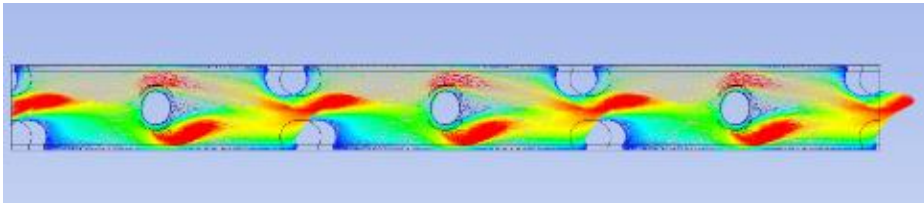

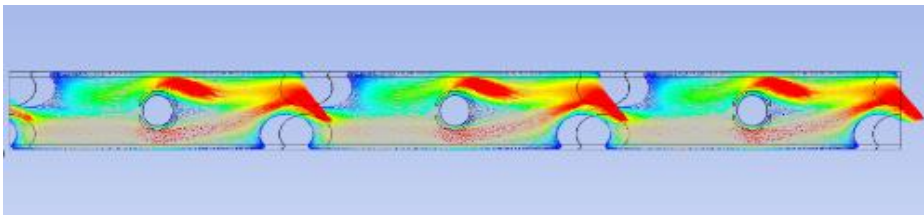**Figure 4.3(a):** Velocity profile for df/hch for middle spacer of 0.3, top and botto
spacer of 0.4
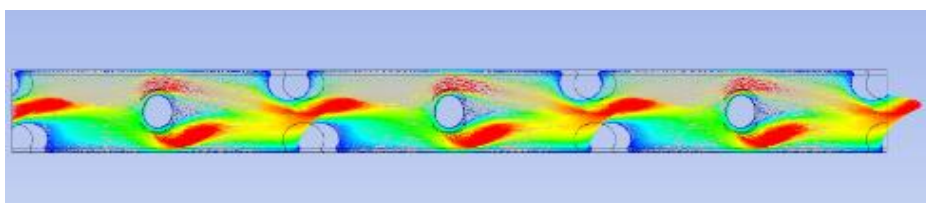
Figure 4.3(b): Velocity profile for df/hch for middle, top and bottom spacer of
0.4

Velocity
Vector 1
6.014e-002

4.511e-002

3.007e-002

1.504e-002

0.000e+000
[m s^-1]
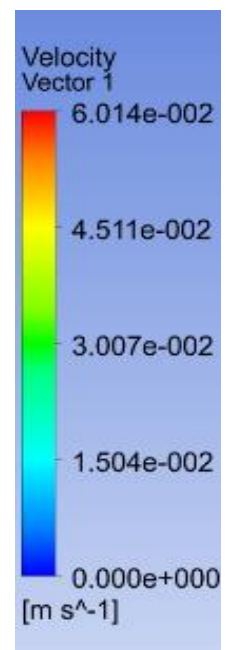
**Figure 4.3(c):** Velocity profile for df/hch for middle spacer of 0.5, top and bottom spacer of 0.4

Figure 4.3(d): Velocity profile for df/hch for middle spacer of 0.4, top and bottom spacer of 0.5

From figure shown above, velocity profile for geometry with middle spacer ratio of 0.3, top and bottom spacer ratio of 0.4 filament give higher velocity compared to other geometry. The velocity consequent follow by the geometry with middle, top and bottom spacer ratio of 0.4, then continue with geometry with middle spacer ratio of 0.5, top and bottom spacer ratio of 0.4 and the lowest velocity was geometry with middle spacer ratio of 0.4, top and bottom spacer ratio of 0.5. This is due to the different spacer size between the edge and the intersection of top, middle and bottom spacer.

An interesting relationship was found for the ratio of volume average of x-vorticity magnitude to volume average of z-vorticity magnitude as seen in figure 4.3(e) for variation in middle size spacer. This ratio was extremely decrease from df/hch middle spacer of 0.3 which is 11.0954 to df/hch of 0.4 which is 0.05384 and slightly increase to 0.09614, df/hch middle spacer of 0.5 .The graph shows that, df/hch for middle spacer of 0.3 have the higher ratio of volume average.
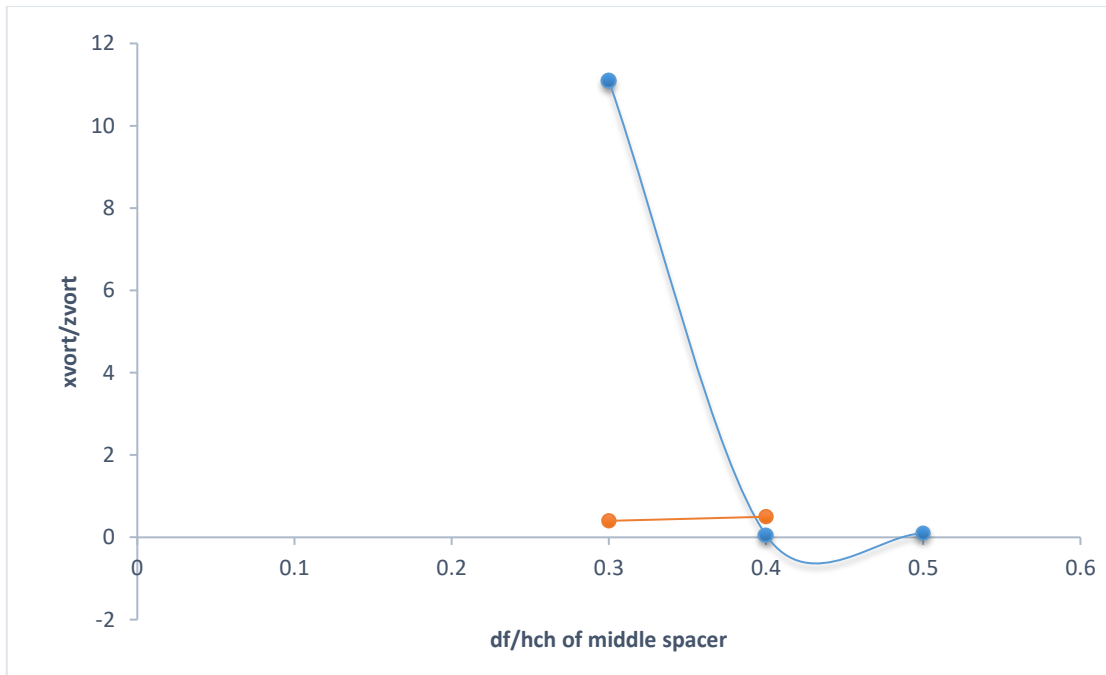
Figure 4.3(e): Ratio of volume average of x-vorticity magnitude to volume average of z-vorticity magnitude for different size of middle spacer.

Besides, when we compared the volume average between different size of top and bottom spacer which are df/hch of 0.4 and 0.5. From the calculation, it shows that geometry with df/hch 0.5 have higher value ratio of volume average which is 2.02599 compared to geometry with df/hch of 0.4 with volume average of 0.05384.
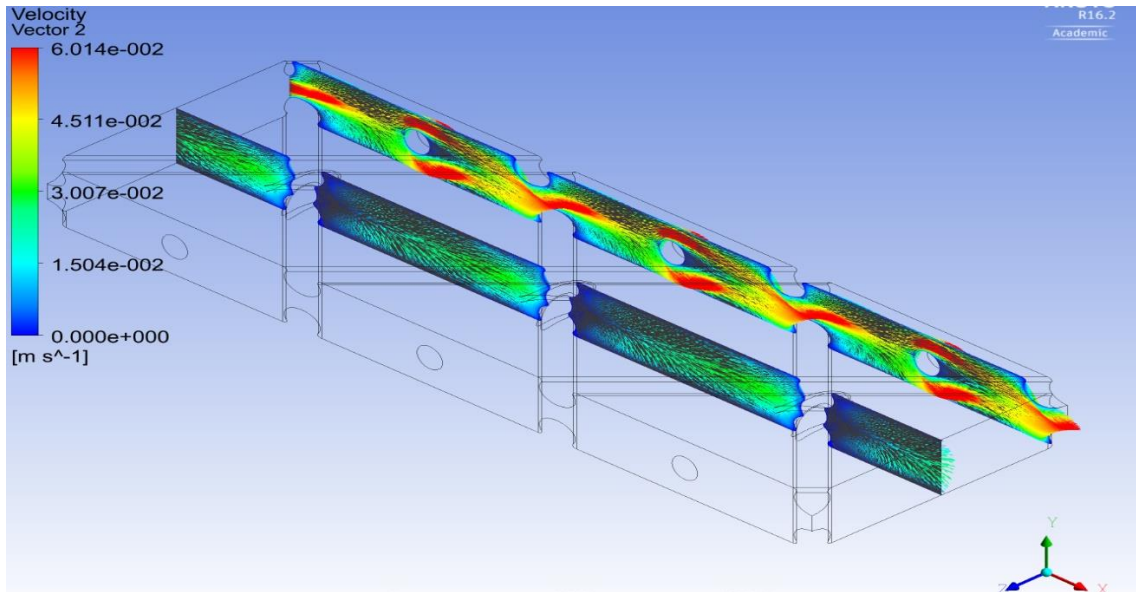
4.4 Effect of Different Size of Spacer on Shear Wall Stress Across the Domain Filaments
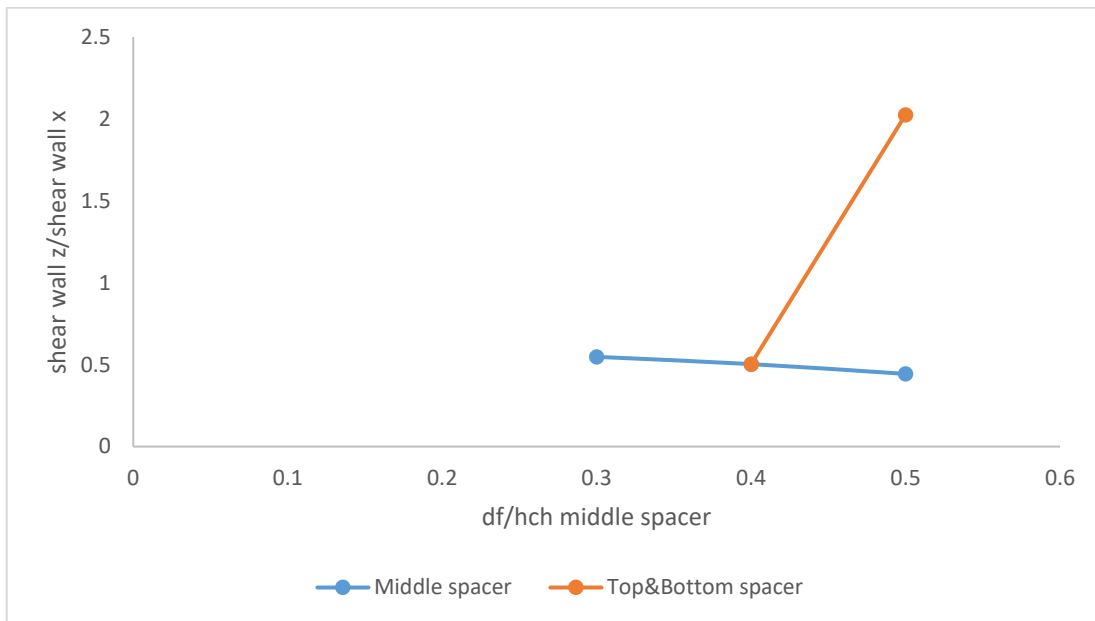
Figure 4.4: Ratio of shear wall stress of shear wall z magnitude to shear wall stress of shear wall x magnitude for different size of middle spacer.

From figure above, the graph shows that the shear wall stress ratio decrease when the df/hch of middle spacer increase. Besides, when we compare the shear wall stress ratio between different df/hch for top and bottom spacer, it shows that as the df/hch larger the shear wall stress ratio will be higher as well.

We want to reduce the concentration polarization through the wall membrane. It can be reduce by enhanced the shear wall stress, then follow by increase the permeate flux of the membrane. Peak value of shear wall stress depends the velocity profile. (Shakaib, Hasani et al. 2009) said that, shear wall stress increase right above the filament and considerably decrease near the centre. Figure 4.4(b) shows the drastic differences between velocity profile of water at centre and near to the interface of the membrane. There are very low movement of water at the centre of the membrane.

**Figure 4.4(b):** Velocity profile at centre and near to the interface.

4.5 Effect of Different Size of Spacer on Fanning Friction Across the Domain Filaments
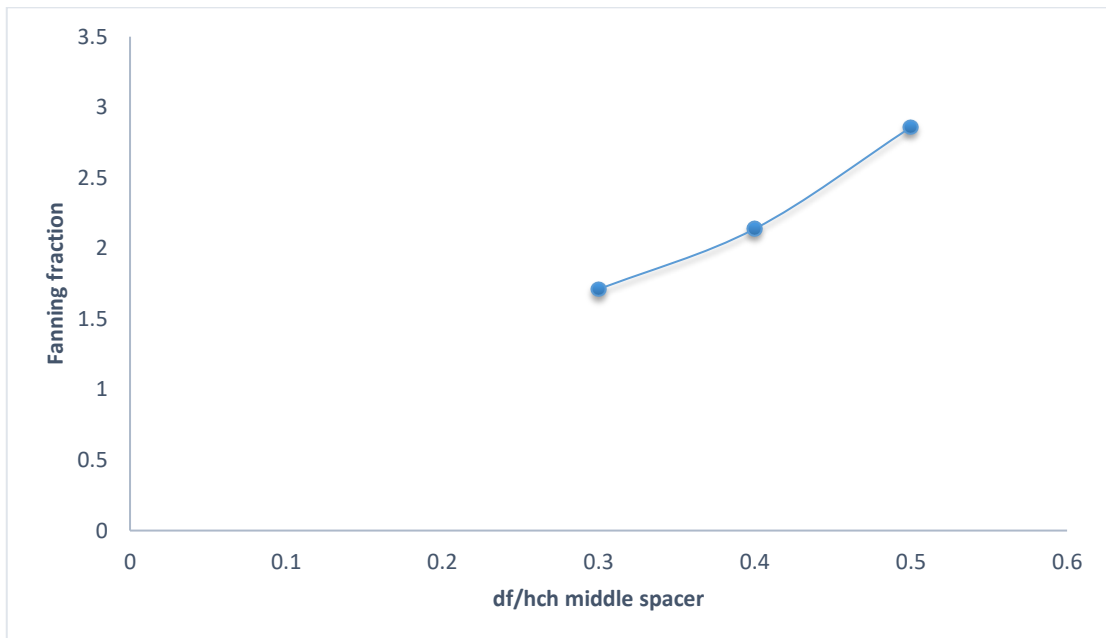
Figure 4.5: Fanning fraction magnitude for different size of middle spacer

From figure 4.5, its shows that the value of fanning fraction increase as the df/hch of middle spacer increase. Besides, fanning fraction also increase if df/hch of top and bottom spacer increase. df/hch of top and bottom spacer of 0.4 give 2.1384 fanning fraction while df/hch of 0.5 give 2.2019 fanning fraction. Thus, we can conclude that the higher the ratio of diameter to height of the spacer the higher the pressure drop. This is supported by (May May Teoh, Sina et al. 2008).

4.6 Effect of Different Size of Spacer on Area Average Fluid Velocity Across the Domain Filaments
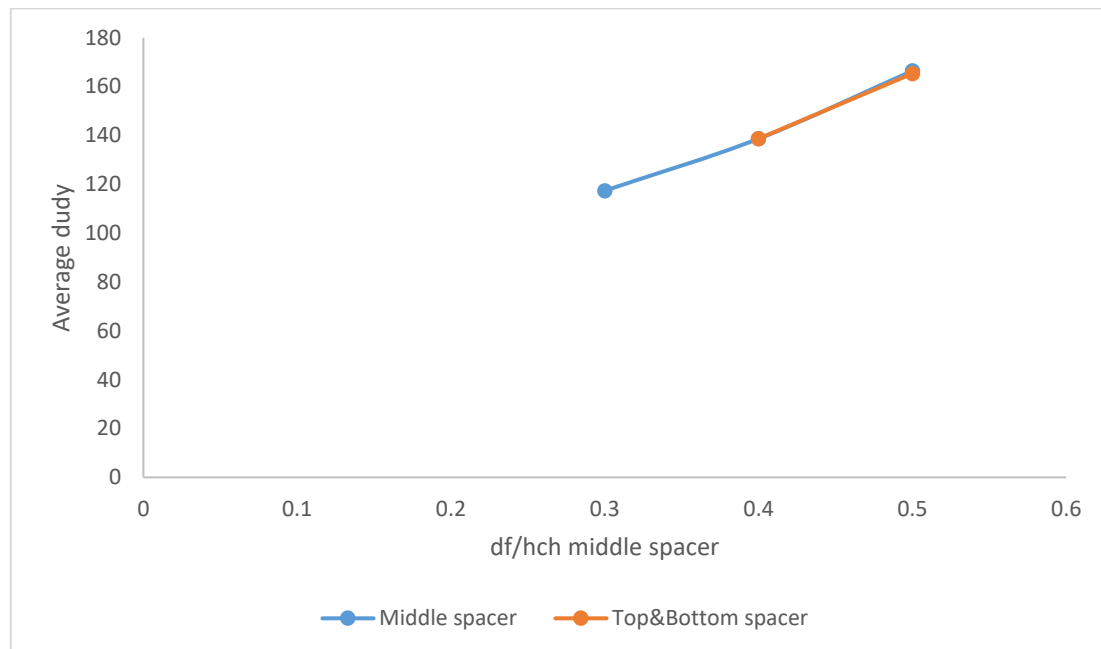
Figure 4.6: Area average fluid velocity of different size of middle spacer

Same as Fanning fraction, area average fluid velocity also have an increment when the df/hch of the spacer of middle top and bottom increase. The df/hch for top and bottom spacer of 0.4 have dudy of 138.66 while df/hch of 0.5 have dudy of 162.21, which indicate that greater spacer size gives greater are average of fluid.

CHAPTER 5

CONCLUSION

In conclusion, there are four cases in this research. We do compared between different middle spacer size and between different top and bottom spacer size. Velocity profile and performance shows that smallest middle spacer size have higher velocity and larger top and bottom spacer size give lower velocity of water. Besides, volume average ratio inclined from df/hch of middle spacer of 0.3 to 0.4 and then has a slightly increase to df/hch 0.5. But it increase when size of top and bottom spacer increase. Moreover, the value for shear wall stress ratio become smaller when the size of middle spacer larger, while if we increase the size of top and bottom spacer, the ratio will increase as well. Furthermore, pressure drop and area average dudy increase as the size of the spacer increase.

REFERENCES

Akhilesh, K. S., M. Srijani, B. Subhankar and A. Perumal (2013). "Spacer layer and temperature driven magnetic properties in multilayer structured FeTaC thin films." Journal of Physics D: Applied Physics **46**(44): 445005.

Amokrane, M., D. Sadaoui, M. Dudeck and C. P. Koutsou (2016). "New spacer designs for the performance improvement of the zigzag spacer configuration in spiral-wound membrane modules." Desalination and Water Treatment **57**(12): 5266-5274.

Balster, J., I. Pünt, D. F. Stamatialis and M. Wessling (2006). "Multi-layer spacer geometries with improved mass transport." Journal of Membrane Science **282**(1–2): 351-361.

Bowen, W. R. and H. Mukhtar (1996). "Characterisation and prediction of separation performance of nanofiltration membranes." Journal of Membrane Science **112**(2): 263-274.

Fimbres-Weihs, G. A. and D. E. Wiley (2007). "Numerical study of mass transfer in three-dimensional spacer-filled narrow channels with steady flow." Journal of Membrane Science **306**(1–2): 228-243.

Fimbres-Weihs, G. A. and D. E. Wiley (2008). "Numerical study of two-dimensional multi-layer spacer designs for minimum drag and maximum mass transfer." Journal of Membrane Science **325**(2): 809-822.

Fimbres-Weihs, G. A. and D. E. Wiley (2010). "Review of 3D CFD modeling of flow and mass transfer in narrow spacer-filled channels in membrane modules." Chemical Engineering and Processing: Process Intensification **49**(7): 759-781.

Fletcher, D. F. and D. E. Wiley (2004). "A computational fluids dynamics study of buoyancy effects in reverse osmosis." Journal of Membrane Science **245**(1): 175-181.

Greenlee, L. F., D. F. Lawler, B. D. Freeman, B. Marrot and P. Moulin (2009). "Reverse osmosis desalination: Water sources, technology, and today's challenges." Water Research **43**(9): 2317-2348.

Hassan, A. M., M. A. K. Al-Sofi, A. S. Al-Amoudi, A. T. M. Jamaluddin, A. M. Farooque, A. Rowaili, A. G. I. Dalvi, N. M. Kither, G. M. Mustafa and I. A. R. Al-Tisan (1998). "A new approach to membrane and thermal seawater desalination processes using nanofiltration membranes (Part 1)." Desalination **118**(1): 35-51.

Karode, S. and C. Anderson (2004). Membrane separation process, Google Patents.

Katsoufidou, K., S. G. Yiantsios and A. J. Karabelas (2007). "Experimental study of ultrafiltration membrane fouling by sodium alginate and flux recovery by backwashing." Journal of Membrane Science **300**(1–2): 137-146.

Kimura, S. (1991). "Characterization of Ultrafiltration Membranes." Polym J **23**(5): 389-397.

Koutsou, C. P. and A. J. Karabelas (2015). "A novel retentate spacer geometry for improved spiral wound membrane (SWM) module performance." Journal of Membrane Science **488**: 129-142.

Koutsou, C. P., S. G. Yiantsios and A. J. Karabelas (2007). "Direct numerical simulation of flow in spacer-filled channels: Effect of spacer geometrical characteristics." Journal of Membrane Science **291**(1–2): 53-69.

Kowalska, I. (2014). "Nanofiltration: ion exchange system for effective surfactant removal from water solutions." Brazilian Journal of Chemical Engineering **31**: 887-894.

Lee, K. P., T. C. Arnot and D. Mattia (2011). "A review of reverse osmosis membrane materials for desalination—Development to date and future potential." Journal of Membrane Science **370**(1–2): 1-22.

Li, F., G. W. Meindersma, A. B. d. Haan and T. Reith (2005). "Novel spacers for mass transfer enhancement in membrane separations." Journal of Membrane Science **253**(1-2): 1-12.

Li, F., W. Meindersma, A. B. de Haan and T. Reith (2002). "Optimization of commercial net spacers in spiral wound membrane modules." Journal of Membrane Science **208**(1–2): 289-302.

Lopes, G. H., B. B. Chavez, N. Ibaseta, P. Guichardon and P. Haldenwang (2012). "Prediction of Permeate Flux and Rejection Rate in RO and NF Membrane Processes: Numerical Modelling of Hydrodynamics and Mass Transfer Coupling." Procedia Engineering **44**: 1934-1936.

Ndinisa, N. V., D. E. Wiley and D. F. Fletcher "Computational Fluid Dynamics Simulations of Taylor Bubbles in Tubular Membranes." Chemical Engineering Research and Design **83**(1): 40-49.

Ochando-Pulido, J. M., V. Verardo, A. Segura-Carretero and A. Martinez-Ferez (2015). "Analysis of the concentration polarization and fouling dynamic resistances under reverse osmosis membrane treatment of olive mill wastewater." Journal of Industrial and Engineering Chemistry **31**: 132-141.

Pasternak, M. (1992). Membrane separation process, Google Patents.

Peng, C. H., H. H. Lee and S. L. Shue (2015). Lithography using multilayer spacer for reduced spacer footing, Google Patents.

Ranade, V. V. and A. Kumar (2006). "Comparison of flow structures in spacer-filled flat and annular channels." Desalination **191**(1): 236-244.

Saeed, A., R. Vuthaluru and H. B. Vuthaluru "Investigations into the effects of mass transport and flow dynamics of spacer filled membrane modules using CFD." Chemical Engineering Research and Design **93**: 79-99.

Schwinge, J., D. E. Wiley and A. G. Fane (2004). "Novel spacer design improves observed flux." Journal of Membrane Science **229**(1–2): 53-61.

Schwinge, J., D. E. Wiley, A. G. Fane and R. Guenther (2000). "Characterization of a zigzag spacer for ultrafiltration." Journal of Membrane Science **172**(1–2): 19-31.

Schwinge, J., D. E. Wiley and D. F. Fletcher (2002). "A CFD study of unsteady flow in narrow spacer-filled channels for spiral-wound membrane modules." Desalination **146**(1): 195-201.

Schwinge, J., D. E. Wiley and D. F. Fletcher (2002). "Simulation of the Flow around Spacer Filaments between Channel Walls. 2. Mass-Transfer Enhancement." Industrial & Engineering Chemistry Research **41**(19): 4879-4888.

Shakaib, M., S. M. F. Hasani and M. Mahmood (2009). "CFD modeling for flow and mass transfer in spacer-obstructed membrane feed channels." Journal of Membrane Science **326**(2): 270-284.

Subramani, A., S. Kim and E. M. V. Hoek (2006). "Pressure, flow, and concentration profiles in open and spacer-filled membrane channels." Journal of Membrane Science **277**(1–2): 7-17.

Tang, C. Y., Q. She, W. C. L. Lay, R. Wang and A. G. Fane (2010). "Coupled effects of internal concentration polarization and fouling on flux behavior of forward osmosis membranes during humic acid filtration." Journal of Membrane Science **354**(1–2): 123-133.

Williams, K. A., S. Saini and T. M. Wick (2002). "Computational Fluid Dynamics Modeling of Steady-State Momentum and Mass Transport in a Bioreactor for Cartilage Tissue Engineering." Biotechnology Progress **18**(5): 951-963.

Shakaib, M., S. M. F. Hasani and M. Mahmood (2009). "CFD modeling for flow and mass transfer in spacer-obstructed membrane feed channels." Journal of Membrane Science 326(2): 270-284.